Journal of Modern Optics
Vol. 57, No. 19, 10 November 2010, 1841–1848

Cooperative scattering by cold atoms

S. Bux[a,b], E. Lucioni[a,c], H. Bender[b], T. Bienaimé[a], K. Lauber[b], C. Stehle[b], C. Zimmermann[b], S. Slama[b], Ph.W. Courteille[a,b,d], N. Piovella[c] and R. Kaiser[a]*

[a]*Institut Non Linéaire de Nice, UMR 6618 CNRS, 1361 route des Lucioles, F-06560 Valbonne, France;* [b]*Physikalisches Institut, Eberhardt-Karls Universität Tübingen, Tübingen D-72076, Germany;* [c]*Dipartimento di Fisica, Università Degli Studi di Milano, Via Celoria 16, Milano I-20133, Italy;* [d]*Instituto de Física de São Carlos, Universidade de São Paulo, 13560-970 São Carlos, SP, Brazil*

(*Received 10 March 2010; final version received 4 June 2010*)

We have studied the interplay between disorder and cooperative scattering for the single scattering limit in the presence of a driving laser. Analytical results have been derived and we have observed cooperative scattering effects in a variety of experiments, ranging from thermal atoms in an optical dipole trap, atoms released from a dark MOT and atoms in a BEC, consistent with our theoretical predictions.

Keywords: cold atoms; Dicke superradiance; cooperative scattering; disorder

1. Introduction

The interaction of quasi-resonant light with a large cloud of atoms has been studied for many years, starting with the seminal work by Dicke [1] and with renewed interest in the context of entanglement which such systems are expected to contain. Often continuous density distributions have been assumed which allow for analytical expressions to be obtained. The role of fluctuations of the atomic density is however by itself at the origin of interesting phenomena, such as Anderson localization of light [2,3]. In a series of theoretical and experimental studies, we have recently addressed the question of the quasi-resonant interaction of light with clouds of cold atoms, bridging the gap from single atom behavior, effects dominated by disorder to a mean field regime, where a continuous density distribution is the relevant description.

In this paper, we present a theoretical model we use to describe the collective atomic response under continuous excitation of a low intensity light field, with additional details compared to [4]. We then present experiments which have been performed in complement to those reported in [5], using atoms in a dipole trap as well as atoms in a magnetic trap, both above and below the Bose–Einstein condensation temperature.

2. Theoretical description

2.1. Hamiltonian and state of the system

We consider a cloud of N two-level atoms (positions $\boldsymbol{r}_j$, lower and upper states $|g_j\rangle$ and $|e_j\rangle$, respectively, transition frequency ω_a, excited state lifetime $1/\Gamma$), excited by a quasi-resonant incident laser propagating along the direction $\hat{\boldsymbol{e}}_z$ (wave vector $\boldsymbol{k}_0$) and with frequency $\omega_0 = \omega_a + \Delta_0$. The atom–field interaction Hamiltonian is in the rotating-wave approximation (RWA) [4][1]

$$\hat{H} = \hbar \sum_{j=1}^{N} \left[\frac{\Omega_0}{2} \hat{\sigma}_j \exp(\mathrm{i}\Delta_0 t - \mathrm{i}\boldsymbol{k}_0 \cdot \boldsymbol{r}_j) + \mathrm{h.c.} \right] + \hbar \sum_{j=1}^{N} \sum_{\boldsymbol{k}} \left[g_k \hat{\sigma}_j \hat{a}_{\boldsymbol{k}}^{\dagger} \exp(\mathrm{i}\Delta_k t - \mathrm{i}\boldsymbol{k} \cdot \boldsymbol{r}_j) + \mathrm{h.c.} \right]. \tag{1}$$

Here, Ω_0 is the Rabi frequency of the interaction between an atom and the classical pump mode, $\hat{\sigma}_j = |g_j\rangle\langle e_j|$ is the lowering operator for atom j, $\hat{a}_{\boldsymbol{k}}$ is the photon annihilation operator, and $g_k = d[\omega_k/(\hbar\epsilon_0 V_{\mathrm{ph}})]^{1/2}$ describes the coupling between the atom and the vacuum modes with volume V_{ph} and frequency $\omega_k = \omega_a + \Delta_k$. We assume that all atoms are driven by the unperturbed incident laser beam, thus neglecting

*Corresponding author. Email: robin.kaiser@inln.cnrs.fr

ISSN 0950–0340 print/ISSN 1362–3044 online

DOI: 10.1080/09500340.2010.503011
http://www.informaworld.com

dephasing by atoms along the laser path or by near field effects, which could arise for large spatial densities. Calling $|0\rangle_a = |g_1, \ldots, g_N\rangle$ the atomic ground state and $|j\rangle_a = |g_1, \ldots, e_j, \ldots, g_N\rangle$ the state where only the atom j is excited, we assume that the total state of the system has the following form [6,7]:

$$|\Psi(t)\rangle = \alpha(t)|0\rangle_a|0\rangle_{\boldsymbol{k}} + \exp(-\mathrm{i}\Delta_0 t)\sum_{j=1}^{N}\tilde{\beta}_j(t) \times \exp(\mathrm{i}\boldsymbol{k}_0\cdot\boldsymbol{r}_j)|j\rangle_a|0\rangle_{\boldsymbol{k}} + \sum_{\boldsymbol{k}}\gamma_{\boldsymbol{k}}(t)|0\rangle_a|1\rangle_{\boldsymbol{k}}. \quad (2)$$

The above expression assumes that only states with at most one atomic excitation contribute to the effects here described.[2]

2.2. *Time evolution of the system*

The time evolution of the amplitudes is obtained by inserting the Hamiltonian (1) and the ansatz (2) into the Schrödinger equation, $\partial_t|\Psi(t)\rangle = -(\mathrm{i}/\hbar)\hat{H}|\Psi(t)\rangle$:

$$\dot{\alpha} = -\frac{\mathrm{i}}{2}\Omega_0\sum_{j=1}^{N}\tilde{\beta}_j, \quad (3)$$

$$\dot{\tilde{\beta}}_j = \mathrm{i}\Delta_0\tilde{\beta}_j - \frac{\mathrm{i}}{2}\Omega_0\alpha - \mathrm{i}\sum_{\boldsymbol{k}} g_k\gamma_{\boldsymbol{k}}\exp[\mathrm{i}(\Delta_0-\Delta_k)t + \mathrm{i}(\boldsymbol{k}-\boldsymbol{k}_0)\cdot\boldsymbol{r}_j], \quad (4)$$

$$\dot{\gamma}_{\boldsymbol{k}} = -\mathrm{i}g_k\exp[-\mathrm{i}(\Delta_0-\Delta_k)t]\sum_{j=1}^{N}\tilde{\beta}_j\exp[-\mathrm{i}(\boldsymbol{k}-\boldsymbol{k}_0)\cdot\boldsymbol{r}_j]. \quad (5)$$

Integrating Equation (5) over time and substituting $\gamma_{\boldsymbol{k}}(t)$ in Equation (4) we obtain:

$$\dot{\tilde{\beta}}_j = \mathrm{i}\Delta_0\tilde{\beta}_j - \frac{\mathrm{i}}{2}\Omega_0\alpha - \sum_{\boldsymbol{k}} g_k^2\sum_{m=1}^{N}\exp[\mathrm{i}(\boldsymbol{k}-\boldsymbol{k}_0)\cdot(\boldsymbol{r}_j-\boldsymbol{r}_m)] \times\int_0^t \mathrm{d}t'\exp[\mathrm{i}(\Delta_0-\Delta_k)(t-t')]\tilde{\beta}_m(t'). \quad (6)$$

Assuming the Markov approximation (valid for $\tau_N \gg \sigma_r/c$, where σ_r is the size of the atomic cloud and τ_N is the cooperative decay time), we can approximate

$$\int_0^t \mathrm{d}t'\exp[\mathrm{i}(\Delta_0-\Delta_k)(t-t')]\tilde{\beta}_m(t') \approx \frac{\pi}{c}\delta(k-k_0)\tilde{\beta}_m(t). \quad (7)$$

Then, going to continuous momentum space via $\sum_{\boldsymbol{k}} \to V_{\mathrm{ph}}(2\pi)^{-3}\int_0^\infty \mathrm{d}k k^2\int \mathrm{d}\boldsymbol{\Omega}_{\boldsymbol{k}}$ (where $\mathrm{d}\Omega_{\boldsymbol{k}} = \sin\theta\ \mathrm{d}\theta\ \mathrm{d}\phi$) and neglecting saturation assuming $\alpha \approx 1$, we obtain

$$\dot{\tilde{\beta}}_j = \mathrm{i}\Delta_0\tilde{\beta}_j - \frac{\mathrm{i}}{2}\Omega_0 - \frac{1}{2}\Gamma\sum_{m=1}^{N}\gamma_{jm}\tilde{\beta}_m, \quad (8)$$

where $\Gamma \equiv (V_{\mathrm{ph}}/\pi c)k_0^2 g_{k_0}^2$ and [8]

$$\gamma_{jm} = \frac{1}{4\pi}\int \mathrm{d}\boldsymbol{\Omega}_{\boldsymbol{k}}\exp[\mathrm{i}(\boldsymbol{k}-\boldsymbol{k}_0)\cdot(\boldsymbol{r}_j-\boldsymbol{r}_m)] = \exp[-\mathrm{i}\boldsymbol{k}_0\cdot(\boldsymbol{r}_j-\boldsymbol{r}_m)]\frac{\sin(k_0|\boldsymbol{r}_j-\boldsymbol{r}_m|)}{k_0|\boldsymbol{r}_j-\boldsymbol{r}_m|}. \quad (9)$$

Due to the presence of the driving term, the solution will evolve quickly toward the driven timed Dicke state [6], characterized by

$$\tilde{\beta}_j(t) = \frac{\beta(t)}{N^{1/2}}. \quad (10)$$

Once inserted the ansatz (10), Equation (8) yields

$$\dot{\beta} = -\frac{\mathrm{i}}{2}N^{1/2}\Omega_0 + \left(\mathrm{i}\Delta_0 - \frac{1}{2}\Gamma N s_N\right)\beta, \quad (11)$$

where

$$s_N = \frac{1}{4\pi}\int_0^{2\pi}\mathrm{d}\phi\int_0^{\pi}\mathrm{d}\theta\sin\theta\left|S_N(k_0,\theta,\phi)\right|^2, \quad (12)$$

and $S_N(\boldsymbol{k}) = (1/N)\sum_{j=1}^{N}\exp[-\mathrm{i}(\boldsymbol{k}-\boldsymbol{k}_0)\cdot\boldsymbol{r}_j]$ is the structure factor of the atomic cloud. In the steady state we find

$$\beta^{\mathrm{st}} \approx \frac{N^{1/2}\Omega_0}{2\Delta_0 + \mathrm{i}N\Gamma s_N}. \quad (13)$$

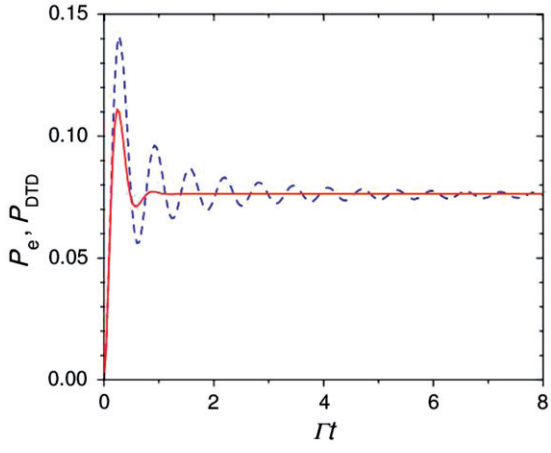

Figure 1. $P_{\mathrm{DTD}}(t) = |\beta(t)|^2$ (red solid line) and $P_e = \sum_j |\tilde{\beta}_j(t)|^2$ (blue dashed line) as a function of Γt obtained using the evolution Equations (11) and (8), respectively. The simulation parameters are $N = 4000$, $\sigma = 10$ for a Gaussian spherical cloud, $\Delta_0 = 10\,\Gamma$ and $\Omega_0 = 0.1\ \Gamma$. (The color version of this figure is included in the online version of the journal.)

In Figure 1 we compare the probability to find atoms in the driven timed Dicke state (10), $P_{\mathrm{DTD}}(t)=|\beta(t)|^2$ (red continuous line) obtained from Equation (11), and the probability that atoms are excited, $P_{\mathrm{e}}(t)=\sum_{j=1}^{N}|\tilde{\beta}_j(t)|^2$ (blue dashed line) obtained solving numerically Equation (8), for a spherical gaussian cloud with $N=4000$ atoms, size $\sigma=k_0\sigma_r=10$ and a pump beam with $\Delta_0=10\Gamma$ and $\Omega_0=0.1\Gamma$. We observe that the exact state tends toward the driven timed Dicke state.

2.3. Forces in the Markov approximation

The two terms in the Hamiltonian (1) yield two different contributions to radiation pressure force:

$$\hat{\boldsymbol{F}}_{\mathrm{a}j}+\hat{\boldsymbol{F}}_{\mathrm{e}j}=-\nabla_{\boldsymbol{r}_j}\hat{H}. \tag{14}$$

We will be interested in the average absorption force, $\boldsymbol{F}_{\mathrm{a}}=N^{-1}\sum_j\langle\hat{\boldsymbol{F}}_{\mathrm{a}j}\rangle$, and emission force, $\boldsymbol{F}_{\mathrm{e}}=N^{-1}\sum_j\langle\hat{\boldsymbol{F}}_{\mathrm{e}j}\rangle$, acting on the center of mass of the whole cloud, $\boldsymbol{F}_{\mathrm{a}}+\boldsymbol{F}_{\mathrm{e}}=m\boldsymbol{a}_{\mathrm{CM}}$, where $\boldsymbol{a}_{\mathrm{CM}}$ is the center-of-mass acceleration and m is the mass of one atom. The first term, $\hat{\boldsymbol{F}}_{\mathrm{a}j}=(\mathrm{i}/2)\hbar\boldsymbol{k}_0\boldsymbol{\Omega}_0[\hat{\sigma}_j\exp(\mathrm{i}\Delta_0 t-\mathrm{i}\boldsymbol{k}_0\cdot\boldsymbol{r}_j)-\mathrm{h.c.}]$ results from the recoil received upon absorption of a photon from the pump laser and has an expectation value on the timed Dicke state (10) given by:

$$\boldsymbol{F}_{\mathrm{a}}=\langle\hat{\boldsymbol{F}}_{\mathrm{a}j}\rangle=-\frac{\hbar k_0\boldsymbol{\Omega}_0}{N^{1/2}}\,\mathrm{Im}[\beta(\mathrm{t})], \tag{15}$$

where we assumed again $\alpha\approx 1$. The second contribution, $\hat{\boldsymbol{F}}_{\mathrm{e}j}=\mathrm{i}\sum_{\boldsymbol{k}}\hbar\boldsymbol{k}g_k[\hat{\sigma}_j\hat{a}_{\boldsymbol{k}}^{\dagger}\exp(\mathrm{i}\Delta_k t-\mathrm{i}\boldsymbol{k}\cdot\boldsymbol{r}_j)-\mathrm{h.c.}]$, results from the emission of a photon into any direction $\boldsymbol{k}$. The expectation value on the general state (2) is:

$$\langle\hat{\boldsymbol{F}}_{\mathrm{e}j}\rangle=\mathrm{i}\sum_{\boldsymbol{k}}\hbar\boldsymbol{k}g_k[\tilde{\beta}_j\gamma_{\boldsymbol{k}}^{*}\exp[-\mathrm{i}(\Delta_0-\Delta_k)t-i(\boldsymbol{k}-\boldsymbol{k}_0)\cdot\boldsymbol{r}_j]-\mathrm{c.c.}]. \tag{16}$$

Substituting the time integral of $\gamma_{\boldsymbol{k}}(t)$ from Equation (5) and inserting the timed Dicke state from Equation (10) we obtain the average emission force:

$$\boldsymbol{F}_{\mathrm{e}}=-\sum_{\boldsymbol{k}}\hbar\boldsymbol{k}g_k^2|S_N(\boldsymbol{k})|^2\left[\beta(t)\int_0^t\mathrm{d}t'\exp[\mathrm{i}(\omega_k-\omega_0)t'\right]\times\beta^{*}(t-t')+\mathrm{c.c.}]. \tag{17}$$

In the Markov approximation and going to continuous momentum space we find

$$\boldsymbol{F}_{\mathrm{e}}=-\hbar\boldsymbol{k}_0\Gamma\left|\beta(t)\right|^2 f_N, \tag{18}$$

where

$$f_N=\frac{1}{4\pi}\int_0^{2\pi}\mathrm{d}\phi\int_0^{\pi}\mathrm{d}\theta\sin\theta\cos\theta\left|S_N(k_0,\theta,\phi)\right|^2. \tag{19}$$

Finally, using Equation (13) in Equations (15) and (18), the average steady-state radiation force acting on the center of mass of the atomic cloud is

$$\boldsymbol{F}_{\mathrm{c}}\equiv\boldsymbol{F}_{\mathrm{a}}+\boldsymbol{F}_{\mathrm{e}}=\hbar\boldsymbol{k}_0\Gamma\frac{N\Omega_0^2}{4\Delta_0^2+N^2\Gamma^2 s_N^2}\,(s_N-f_N). \tag{20}$$

The common prefactor can be obtained from the standard low saturation single-atom radiation force $\boldsymbol{F}_1=\hbar\boldsymbol{k}_0\Gamma\boldsymbol{\Omega}_0^2/(4\Delta_0^2+\Gamma^2)$ by substituting the natural linewidth by the collective linewidth, $\Gamma\to N\Gamma\, s_N$, and the Rabi frequency by the collective Rabi frequency, $\Omega_0\to N^{1/2}\,\Omega_0$. Additionally, the cooperative radiation pressure force is weighted by the difference of structure factors, s_N-f_N, where the s_N part corresponds to the cooperative absorption process and the f_N part to the cooperative emission. For smooth density distributions $n(\boldsymbol{r})$, one could compute the structure functions by replacing the sum with an integral ($s_N\to s_\infty$ and $f_N\to f_\infty$). However, we have shown [5] that in this way we miss the role of the disorder in the atomic positions r_j in the scattering process and the crossover from single atom radiation force and cooperative scattering. Instead, estimating the fluctuations of s_N and f_N one finds that (see Figure 2(*a*)):

$$s_N\approx\frac{1}{N}+s_\infty,\quad f_N\approx f_\infty. \tag{21}$$

Using (21), the ratio between the cooperative radiation force (20) and the single atom force is

$$\frac{F_{\mathrm{c}}}{F_1}=\frac{4\Delta_0^2+\Gamma^2}{4\Delta_0^2+\Gamma^2(1+Ns_\infty)^2}[1+N(s_\infty-f_\infty)]. \tag{22}$$

Assuming a smooth Gaussian density distribution with ellipsoidal shape, $n_0\exp[-(x^2+y^2)/2\sigma_r^2-z^2/2\sigma_z^2]$, the structure factor is $S_\infty(k_0,\ \theta,\ \phi)=\exp\{-\sigma^2[\sin^2\theta+\eta^2(\cos\theta-1)^2]/2\}$, where $\sigma=k_0\sigma_r$ and $\eta=\sigma_z/\sigma_r$ is the aspect ratio. For elongated clouds, $\eta\geq 1$,

$$s_\infty^{(\eta)}=\frac{\pi^{1/2}\exp[\sigma^2/(\eta^2-1)]}{4\sigma(\eta^2-1)^{1/2}}\left\{\mathrm{erf}\left[\frac{\sigma(2\eta^2-1)}{(\eta^2-1)^{1/2}}\right]-\mathrm{erf}\left[\frac{\sigma}{(\eta^2-1)^{1/2}}\right]\right\},$$

$$f_\infty^{(\eta)}=\frac{1}{\eta^2-1}\left[\eta^2 s_\infty^{(\eta)}-\frac{1}{4\sigma^2}\left[1-\exp\left(-4\eta^2\sigma^2\right)\right]\right]. \tag{23}$$

For spherical clouds ($\eta=1$) and for $\sigma\gg 1$ one finds $s_\infty\approx 1/4\sigma^2$ and $s_\infty-f_\infty\approx 1/8\sigma^4$. For $\sigma,\ \eta\gg 1$, $s_\infty^{(\eta)}$ can be approximated by $s_\infty^{(\eta)}\simeq s_\infty\pi^{1/2}F\exp(F^2)[1-\mathrm{erf}(F)]$, where $F\equiv\sigma/\eta=k\sigma_r^2/\sigma_z$ is the Fresnel number. For large Fresnel numbers $s_\infty^{(\eta)}\to s_\infty$.

As illustrated by Figure 2(*b*), the single-atom force is recovered in the limit of $N\,s_\infty\sim N/4\sigma^2\ll 1$, i.e. for

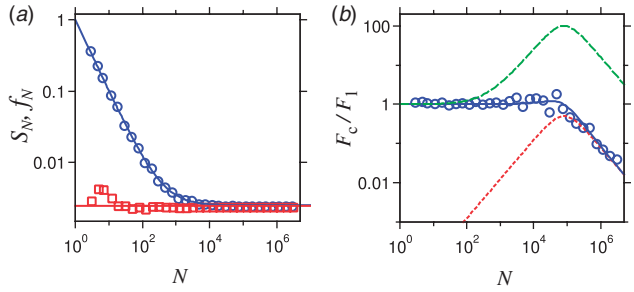

Figure 2. Analytical expressions and numerical evaluation for $\sigma = 10$ with a configuration average on 10 realizations as a function of atom number. (*a*) Results for s_N (blue circles), f_N (red squares) and analytical expressions $1/N + s_\infty$ (blue line), f_∞ (red line). (*b*) Forces acting on a cloud of atoms with $\Delta_0 = -100\,\Gamma$: numerical evaluation (blue circles) of the average cooperative force. The full lines indicate (i) the force in the presence of isotropic scattering, i.e. assuming $f_N = 0$ (green dashed line), (ii) the force for continuous density distributions without disorder (red dotted line) and (iii) the total force taking into account cooperative scattering and disorder in the atomic positions r_j (blue line). (The color version of this figure is included in the online version of the journal.)

small optical thickness $b_0 \approx 3N/\sigma^2$. Conversely, for large b_0 the microscopic inhomogeneities can be neglected and cooperativity strongly modifies the radiation force. In particular, for small volumes the emission is isotropic and $f_\infty \approx 0$, whereas for large volumes the recoil at the emission compensates the recoil at absorption, $f_\infty \approx s_\infty$, which results in mainly forward emission.

3. Experimental results

The analytical results presented in the previous section should apply to a large variety of clouds of cold atoms, including thermal cold atoms as well as degenerate quantum gases (as long as atom–atom interactions can be neglected). In this section we report first observations of cooperative scattering in different regimes: thermal clouds in a dipole trap or released from a dark MOT and for a Bose–Einstein condensate realized from a magnetic trap.

3.1. *Thermal cold atoms in a dipole trap*

A first series of experiments were performed in Nice in 2008, where we were looking for possible signatures related to collective atomic recoil lasing (CARL), with spontaneous atomic bunching, when a large cloud of atoms is exposed to off-resonant detuned light. In contrast to previous experiments [9], this setup does not use a high finesse cavity, but the larger atom number we are able to trap [10] might allow one to compensate for the absence of the cavity. The results of these studies did not show any evidence of CARL, but provided the first signatures of cooperative scattering. The experiment was performed using a vapor-loaded magneto-optical trap (MOT) of ^{85}Rb atoms. The cooling laser was derived from a distributed

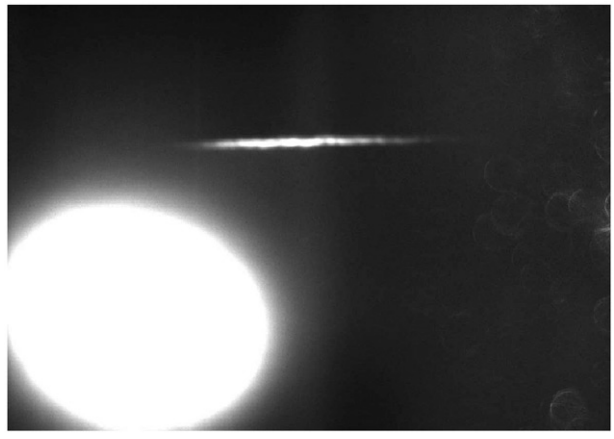

Figure 3. Fluorescence image of the cold atoms. The large cloud corresponds to the free falling atoms and the narrow cigar shaped cloud to atoms trapped in the focus of the dipole laser beam.

feedback-laser (DFB) master laser amplified by a tapered amplifier (TA), whereas the repump laser was a simple DFB laser. After a dark MOT period of 35 ms, we loaded the atoms into a red detuned single beam dipole trap, formed by another DFB laser amplified by a TA and focused to a beam waist of $\approx$200 µm. The action of this dipole trap laser is twofold: on one side it holds atoms against gravity due to the dipole forces and, on the other side, as the atom–laser detuning is not very large, the residual radiation pushes the atoms along the dipole trap. As one can see in Figure 3 most of the atoms of the dark MOT are not loaded into the dipole trap and fall under the action of gravity. A small fraction of the atoms are however trapped in the dipole laser beam and are pushed along the axes of propagation of the laser. This observation is not surprising, given the moderate detuning (at least for dipole traps) we have used,

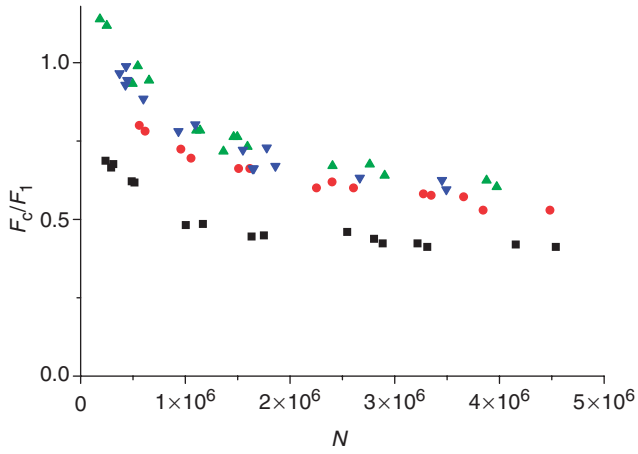

Figure 4. Average radiation force on the cloud of the atoms. For increasing atom number, the cloud is less displaced by the dipole laser. The interaction time for this experiment is 50 ms, the laser beam power is 100 mW for $\Delta_0 = -76$ GHz (black square), $\Delta_0 = -87$ GHz (red circles), $\Delta_0 = -90$ GHz (green triangles) and $\Delta_0 = -108$ GHz (blue stars). (The color version of this figure is included in the online version of the journal.)

with values ranging from $\Delta_0 = -50$ GHz to $\Delta_0 = -200$ GHz (detuning Δ_0 given with respect to the $F = 3 \rightarrow F' = 4$ transition of the D2 line of ^{85}Rb). This regime of dipole traps where radiation pressure cannot be neglected is not commonly studied, as spontaneous scattering of photons is usually not desired. The experimental protocol using the dipole trap to both hold the atoms against gravity and push them with off-resonant radiation pressure made it difficult to independently change the parameters for the dipole trap (and thus the size and shape of the atomic cloud) and for the radiation pressure effects. This experiment, however, provided our first signatures of cooperative scattering which were studied later on in a more quantitative way. We thus show in this section our first qualitative results, which could not be compared in a quantitative way to a theoretical model. As this experimental protocol required a finite interaction time in the dipole trap in order to allow separation of the untrapped and trapped atoms, the shape of the cloud of atoms changes during this interaction time. This further complicates a reliable comparison to the theoretical model.

In Figure 4 we plot the average force acting on the center of mass of the cloud of atoms kept in the dipole trap. This force can be extracted from the spatial displacement, as the interaction time is well known. The normalization of the force to the single atom force is roughly estimated from the measured values of laser power and detuning. The most striking point to notice in Figure 4 is the clear reduction of the average radiation force with increasing atom number. This effect has been subsequently studied in a quantitative way [5].

During the course of these experiments, we have observed some intriguing features which have not yet been studied in a quantitative way. For instance we found a systematic oscillation of the average radiation pressure force, as illustrated in Figure 5. These oscillations turned out to be very robust and above shot-to-shot fluctuations which in such experiments are of the order of 2.5% for the displacement of the center of mass. This feature clearly merits further experimental investigation, since if it is not due to an experimental artefact, it might be related to effects beyond the Markhov approximation, where ringing of superradiant time decay is predicted [7].

3.2. *Thermal cold atoms released from a dark MOT*

Following the first series of experiments and the development of our theoretical model presented above, we performed experiments which allowed for a quantitative comparison. The main results of these experiments have been presented in [5] and we thus only show the main result here. These experiments have been done using the same vapor cell as in the previous experiments. These new results have, however, used the ^{87}Rb isotope. The experimental protocol used to allow for a quantitative measurement of cooperative scattering did not use atoms in a dipole trap, but atoms released from a dark MOT. Adapting the number of atoms interacting with the pushing laser by controlled repumping from the $F = 1$ to the $F = 2$ hyperfine level in the ground state, we changed the optical thickness of the cloud without changing the size of the cloud. This allowed for a quantitative measurement of the radiation force as illustrated in Figure 6.

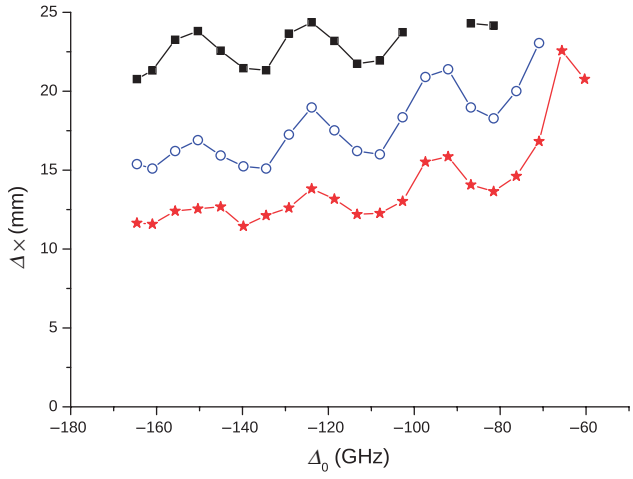

Figure 5. Displacement of the center of mass of the atomic cloud as a function of detuning for different interaction times: 50 ms (red stars), 60 ms (open blue circles), 70 ms (black squares) obtained for a laser power of $P = 100$ mW. (The color version of this figure is included in the online version of the journal.)

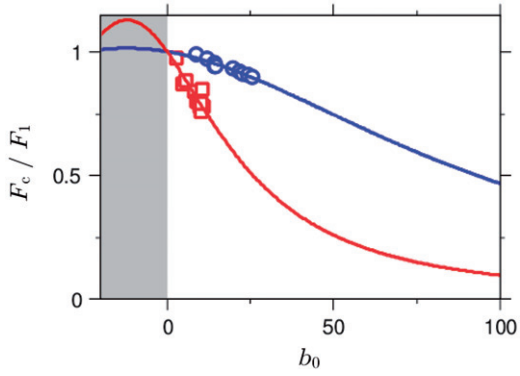

Figure 6. Experimental data and fits using the cooperative radiation force F_c (normalized to the single atom radiation force F_1) in the presence of disorder for $\Delta_0 = -1.9\,\Gamma$ (red squares) and $\Delta_0 = -4.2\,\Gamma$ (blue circles). The shadowed area corresponds to the non-physical region $b_0 < 0$. (The color version of this figure is included in the online version of the journal.)

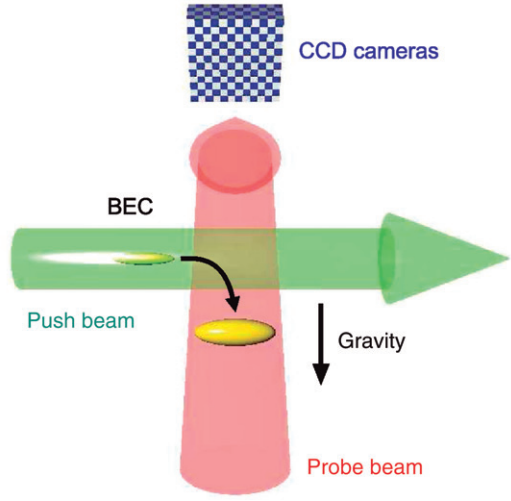

Figure 7. Scheme of the experiment. (The color version of this figure is included in the online version of the journal.)

We take the good agreement between experiments and theory as a proof of the relevance of cooperative scattering in clouds of cold atoms.

3.3. *Measurements in a magnetic trap*

The experiment described above presents the first clean signatures of cooperative scattering of single photons along the lines of the model outlined in [4,6,7]. At the large pump laser detunings and the large cloud volumes used, the light was strongly scattered in the forward direction. In the case of small volumes, the absorbed light can be re-emitted in directions other than the forward one. Cooperativity then also leaves its imprint in the geometry of the radiation pattern.

Particularly small and dense samples can be made by cooling the atomic cloud to ultralow temperatures. Ultimately, their size is limited by the repulsive interatomic interaction making it difficult to reach sample sizes on the order of $\sigma \simeq 1$. Another advantage of samples with temperatures below the recoil limit is that the interaction with a light field leaves detectable traces in their momentum distribution even when, on average, every atom scatters much less than a single photon.

In an experiment performed at the University of Tübingen we prepare a ^{87}Rb cloud in a magnetic trap

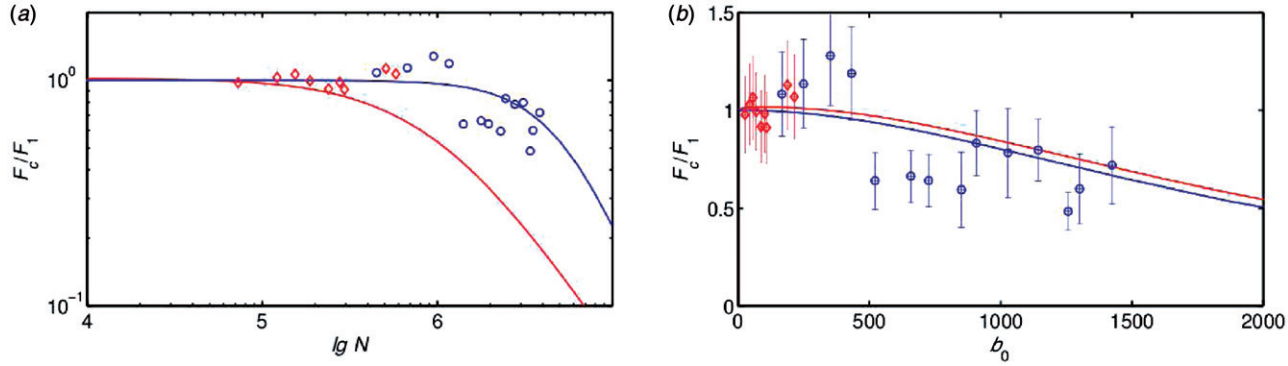

Figure 8. Blue lines and blue circles correspond to $T = 1\,\mu$K cold thermal clouds (size and shape independent of N), red lines and red diamonds to condensates in the Thomas–Fermi limit (size and shape depend on N). (*a*) Calculated (lines) and measured (symbols) N-dependence of the radiation pressure ratio. (*b*) Same as (*a*), but in linear scales and as a function of resonant optical density. The experimental parameters were $\Delta_0 = 500$ MHz, σ_+-pol, $\tau_0 = 20\,\mu$s, $\tau_{\rm tof} = 20$ ms. No parameters were adjusted. Every data point is an average over several measurements. The error bars shown in the linear plot (*b*) arise from statistical fluctuations of the measured radiation pressure force and an estimated uncertainty of the push beam intensity of 20%. (The color version of this figure is included in the online version of the journal.)

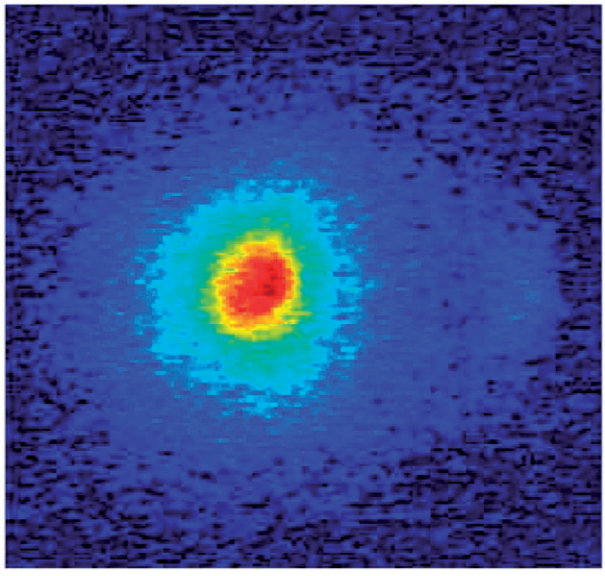

Figure 9. Absorption images of an atomic cloud released from the magnetic trap. Due to the scattering the momentum distribution is slightly deformed and develops a tiny peak visible on the right side of the image. (The color version of this figure is included in the online version of the journal.)

and cool it down by forced evaporation to quantum degeneracy. The trap is ellipsoidal with frequencies $\omega_z = 25$ Hz and $\omega_r = 160$ Hz. We now apply in the axial direction a light pulse with a power of $P_0 = 130\,\mu$W and a diameter of $\omega_0 = 295\,\mu$m for a duration of $\tau_0 = 10 \ldots 500\,\mu$s detuned from the D2 line by $\Delta_0 = 500$ MHz. Immediately after the pulse (within 100 μs) the trap is switched off. The cloud falls in free expansion for $t_{\rm tof} = 20$ ms before we apply an imaging pulse in the transversal (radial) direction (see Figure 7).

We either use thermal clouds of $N = 10^5 \ldots 4 \times 10^6$ atoms at a temperature of $T \simeq 1\,\mu$K or Bose–Einstein condensates of $N = 10^4 \ldots 6 \times 10^5$ atoms. In the case of thermal clouds the aspect ratio is $\eta = 5.6$ and the size is $\sigma = 90$, independent on N (see Figure 8). In the case of a condensate the interatomic interaction gives rise to a chemical potential of up to $\mu/h = 10$ kHz and a transverse radius in the Thomas–Fermi limit of up to $\sigma = 60$. Also the aspect ratio depends on the atom number, because the mean field presses the condensate into the weakly confining dimension. Optical densities of up to $b_0 = 2000$ are reached in the axial direction.

The effective radiation pressure is extracted from time-of-flight absorption images such as the one shown in Figure 9. The first moment of the momentum distribution $\Delta p = m\Delta z_{cm}/t_{\rm tof}$ is a measure for the collective radiation force. The tendency of the radiation force to decrease with increasing atom number is clearly visible and will be subject to future investigations.

4. Conclusion

Cooperative effects in scattering of light by large clouds of cold atoms present phenomena which can be described by using driven timed Dicke states. These states present a convenient quantum approach even though the features exploited in the present paper do not go beyond what can be expected from a classical treatment. We have given detailed results on our theoretical model, with an analytical expression for the modified radiation force when large clouds of atoms are used. Experimental confirmation of the

modification of the radiation force has been observed in two different laboratories using different experimental configurations, ranging from cold atoms held in an optical dipole trap, atoms released from a dark MOT to atoms in a BEC setup with a magnetic trap. These experiments illustrate the wide range of situations where such cooperative scattering processes need to be considered. Important future extensions of this work arising from these cooperative processes would include any possible 'quantum' feature which could not be described with classical models. Fluctuations and higher order correlations seem appropriate first signatures to study in this respect.

Acknowledgements

This work has been supported by ANR (Project nos. ANR-06-BLAN-0096 and ANR-09-JCJC-009401), DFG (Contract no. Co 229/3-1), DAAD and INTERCAN.

Notes

1. A debate has been brought up concerning the validity of the RWA in the regime, where collective Lamb shifts may play a role [11].
2. The presence of many excitations in the cloud means that higher Dicke states are populated. Then we may expect a complicated many-body dynamics, if decay into other states than the timed Dicke state is possible.

References

[1] Dicke, R.H. *Phys. Rev.* **1954,** *93,* 99–110.
[2] Akkermans, E.; Gero, A.; Kaiser, R. *Phys. Rev. Lett.* **2008,** *101,* 103602.
[3] Sokolov, I.M.; Kupriyanova, M.D.; Kupriyanov, D.V.; Havey, M.D. *Phys. Rev. A* **2009,** *79,* 053405.
[4] Courteille, Ph.W.; Bux, S.; Lucioni, E.; Lauber, K.; Bienaime, T.; Kaiser, R.; Piovella, N. *Eur. Phys. J. D* **2010,** *58,* 69–73.
[5] Bienaimé, T.; Bux, S.; Lucioni, E.; Courteille, Ph.W.; Piovella, N.; Kaiser, R. *Phys. Rev. Lett.* **2010,** *104,* 083602.
[6] Scully, M.O.; Fry, E.S.; Ooi, C.H.R.; Wodkiewicz, K. *Phys. Rev. Lett.* **2006,** *96,* 010501.
[7] Svidzinsky, A.A.; Chang, J.-T.; Scully, M.O. *Phys. Rev. Lett.* **2008,** *100,* 160504.
[8] Scully, M.O.; Svidzinsky, A.A. *Phys. Lett. A* **2009,** *373,* 1283–1286.
[9] Kruse, D.; von Cube, Ch.; Zimmermann, C.; Courteille, Ph.W. *Phys. Rev. Lett.* **2003,** *91,* 183601.
[10] Labeyrie, G.; Michaud, F.; Kaiser, R. *Phys. Rev. Lett.* **2006,** *96,* 023003.
[11] Friedberg, R.; Manassah, J.T. *Phys. Lett. A* **2008**, *372*, 2514–2521; Svidzinsky, A.A.; Chang, J.-T. *ibid.* **2008**, *372*, 5732–5733; Friedberg, R.; Manassah, J.T. *ibid.* **2008**, *372*, 5734–5740.